

# In-Tube DNA Methylation Profiling by Fluorescence Melting Curve Analysis

JESPER WORM,<sup>1</sup> ANNI AGGERHOLM,<sup>2</sup> and PER GULDBERG<sup>1\*</sup>

**Background:** Most PCR assays for detection of 5-methylcytosine in genomic DNA entail a two-step procedure, comprising initial PCR amplification and subsequent product analysis in separate operations that usually require manual transfer. These methods generally provide information about methylation of only a few CpG dinucleotides within the target sequence.

**Methods:** An in-tube methylation assay is described that integrates amplification of bisulfite-treated DNA and melting analysis by using a thermal cycler coupled to a fluorometer (LightCycler). DNA melting curves were acquired by measuring the fluorescence of a double-stranded DNA-binding dye (SYBR Green I) during a linear temperature transition.

**Results:** Analysis of a region comprising 11 CpG sites at the *SNRPN* promoter CpG island showed that the melting temperature ( $T_m$ ) differed by  $\sim 3$  °C between unmethylated and fully methylated alleles. This assay could easily distinguish patients with Prader-Willi syndrome or Angelman syndrome from individuals without these conditions. Melting curve analysis also allowed resolution of methylation "mosaicism" at the *p15<sup>Ink4b</sup>* promoter in bone marrow samples from patients with acute myeloid leukemia (AML). AML samples representing pools of heterogeneously methylated *p15<sup>Ink4b</sup>* alleles showed broadened melting peaks with overall  $T_m$ s between those of the unmethylated and fully methylated alleles.

**Conclusions:** Integration of PCR and fluorescence melting analysis may be useful for simple and cost-effective detection of aberrant methylation patterns.

© 2001 American Association for Clinical Chemistry

5-Methylcytosine ( $m^5C$ )<sup>3</sup> occurs in the context of CpG dinucleotides and is the most abundant covalently modified base in the genomes of vertebrates. Areas of high CpG dinucleotide density, so called "CpG islands", are spread throughout the genomes and usually map to gene-promoter regions. Methylation of promoter CpG islands is associated with histone deacetylation and transcriptional silencing (1) and is essential for normal embryonic development, genomic imprinting, and X-chromosome inactivation. Somatic de novo methylation of CpG islands in tumor suppressor genes has been implicated in tumorigenesis, and aberrant methylation of imprinted genes is associated with several inherited human diseases (1–3). The central role of DNA methylation in normal and disease-related processes has led to a variety of methods to detect and characterize normal and aberrant methylation patterns in biologic and clinical specimens.

In standard PCR and cloning procedures, information about  $m^5C$  and other covalent base modifications in genomic DNA is lost. Therefore, current PCR methods for detecting and mapping  $m^5C$  in specific genes rely on treatment of genomic DNA with methylation-sensitive restriction endonucleases or sodium bisulfite before amplification. Bisulfite converts unmethylated cytosines to uracil, whereas methylated cytosines remain unreactive (4). A specific target sequence can subsequently be amplified with primers specific for bisulfite-converted DNA and examined for its  $m^5C$  content. The gold standard among bisulfite methods is genomic sequencing that provides a positive display of  $m^5C$  at specific CpG sites in virtually any stretch of DNA (5). More simple methods using bisulfite-converted DNA as a template include methylation-specific PCR (MSP) (6), methylation-sensitive single nucleotide primer extension (7) and procedures based on the use of restriction endonucleases (8, 9).

<sup>1</sup> Department of Tumor Cell Biology, Institute of Cancer Biology, Danish Cancer Society, Strandboulevarden 49, DK-2100 Copenhagen, Denmark.

<sup>2</sup> Department of Haematology, Aarhus University Hospital, Tage-Hansens Gade 2, DK-8000 Aarhus C, Denmark.

\*Author for correspondence. Fax 45-35-25-77 21; e-mail perg@cancer.dk.

Received December 12, 2000; accepted April 6, 2001.

<sup>3</sup> Nonstandard abbreviations:  $m^5C$ , 5-methylcytosine; MSP, methylation-specific PCR;  $T_m$ , melting temperature; AML, acute myeloid leukemia; and SNRPN, small nuclear ribonucleoprotein-associated polypeptide N.

Despite the obvious advantages of the above methods, they all entail a two-step procedure, comprising initial PCR amplification and subsequent product analysis, usually by gel electrophoresis. Furthermore, with the exception of genomic sequencing, they are limited to the analysis of one or a few CpG sites in each setting. We describe a new in-tube PCR assay for the detection of aberrant DNA methylation that uses a thermal cycler integrated with a fluorometer (10) and exploits differences in melting temperature ( $T_m$ ) between methylated and unmethylated alleles after bisulfite treatment.

## Materials and Methods

### DNA SAMPLES

Mononuclear cells were obtained from peripheral blood from patients with Angelman syndrome or Prader-Willi syndrome and apparently healthy individuals, or from bone marrow from patients with acute myeloid leukemia (AML). Genomic DNA was isolated using the Puregene DNA Isolation Kit (Gentra Systems). DNA from the leukemia cell lines, MOLT-4 and HL-60, served as the positive and negative controls for  $p15^{\text{Ink4b}}$  methylation (11), respectively. Blood and bone marrow samples were obtained after informed consent, and all procedures were in accordance with the current revision of the Helsinki Declaration of 1975.

### SODIUM BISULFITE CONVERSION

Genomic DNA was treated with sodium bisulfite essentially as described previously (12). Briefly,  $\sim 2 \mu\text{g}$  of DNA was denatured in 0.3 mol/L NaOH for 15 min at 37 °C, followed by the addition of sodium bisulfite to a final concentration of 3.1 mol/L and hydroquinone to a final concentration of 2.5 mmol/L. After incubation at 55 °C for 16 h, the DNA samples were recovered using the GeneClean II Kit (Bio 101 Inc.), desulfonated in 0.3 mol/L NaOH, and ethanol-precipitated. DNA was resuspended in Tris-EDTA and used immediately or stored at  $-80 \text{ }^\circ\text{C}$  until use.

### PRIMER DESIGN AND PCR AMPLIFICATION

Melt maps were generated using the MELT94 algorithm (13). Primers specific for bisulfite-converted antisense DNA were selected to amplify a region of the small nuclear ribonucleoprotein-associated polypeptide N (SNRPN) gene promoter CpG island (GenBank Accession No. L32702; bases 153–305). This region is within the area known to be methylated differentially in the Angelman and Prader-Willi syndromes (14). The primers were SNRPN-A [(CGGGCGGGG)-CATACTCAAATAAA-ATATACTAAACCTACC] and SNRPN-B [(CGCCCGCCCGCGCCCGTCCCGCCCGCCCGCCCG)-AGAGAAGTTATTGGTATAGTTGATTTTGTT]. Nucleotides in parentheses represent GC-clamps. Primers for amplification of the  $p15^{\text{Ink4b}}$  promoter CpG island were described previously (11). PCR was carried out in a final volume of 25  $\mu\text{L}$  containing 100–200 ng of bisulfite-

treated DNA, 10 mM Tris-HCl (pH 8.3), 50 mM KCl, 1.5 mM  $\text{MgCl}_2$ , 0.2 mM dNTP, 0.4  $\mu\text{M}$  each primer, and 1 U of AmpliTaq polymerase (Perkin-Elmer). PCR was initiated by hot-start, followed by 39 cycles of 94 °C for 30 s, 55 °C for 30 s and 72 °C for 30 s, and a final extension at 72 °C for 5 min, using a block thermocycler (GeneAmp PCR System 9600; Perkin-Elmer). PCR products were examined by electrophoresis on 2–3% agarose gels (FMC).

For amplification on the LightCycler (Roche), a LightCycler DNA Master SYBR Green I reagent set (Roche) was used. Before amplification, 2  $\mu\text{L}$  of 10 $\times$  LightCycler DNA Master SYBR Green I was mixed with 0.16  $\mu\text{L}$  of TaqStart Antibody (Clontech) and incubated at room temperature for 5 min. PCR was performed in 20- $\mu\text{L}$  reactions containing 2  $\mu\text{L}$  of 10 $\times$  LightCycler DNA Master SYBR Green I, 3 mM  $\text{MgCl}_2$ , 200 ng of bisulfite-treated DNA, and 0.5  $\mu\text{M}$  each primer. PCR was initiated by incubation for 1 min at 95 °C to denature the TaqStart Antibody, followed by 40–50 cycles of 5 s at 95 °C, 10 s at 55 °C, and 15 s at 72 °C. The fluorescence of SYBR Green I was measured once per cycle to monitor template amplification.

### GENERATION OF MELTING CURVES AND MELTING PEAKS

DNA melting curves were acquired on the LightCycler by measuring the fluorescence of SYBR Green I during a linear temperature transition from 70 °C to 98 °C at 0.1 °C/s. Fluorescence data were converted into melting peaks by the LightCycler software (Ver. 3.39) to plot the negative derivative of fluorescence over temperature vs temperature ( $-dF/dT$  vs  $T$ ). For PCR products generated on a block thermocycler, 5  $\mu\text{L}$  of PCR product was mixed with 5  $\mu\text{L}$  of a 1:5000 dilution of SYBR Green I (Molecular Probes) and 10  $\mu\text{L}$  of  $\text{H}_2\text{O}$  before melting curve analysis. For PCR products generated on the LightCycler, melting curve analysis was performed immediately after amplification.

## Results

### RATIONALE OF MELTING CURVE ANALYSIS FOR DNA METHYLATION PROFILING

When a double-stranded DNA molecule is subjected to gradual heating, it melts in a series of steps, in which each step represents the melting of a discrete segment, a so-called “melting domain”. In general, the  $T_m$  of a melting domain increases with an increase in GC content. After conversion of unmethylated cytosines to uracil by sodium bisulfite and subsequent PCR-mediated conversion of uracils to thymine, methylated and unmethylated alleles are predicted to differ in thermal stability because of their different GC contents (15).

As shown schematically in Fig. 1, the  $T_m$  of an amplification product is determined by the composition of methylated and unmethylated alleles in the original DNA sample. If all alleles are completely devoid of  $\text{m}^5\text{C}$ , all cytosines will be converted to thymine, yielding a PCR product with a relatively low  $T_m$  (Fig. 1A). By contrast, if all alleles contain  $\text{m}^5\text{C}$  at all CpG dinucleotides, the  $T_m$  of

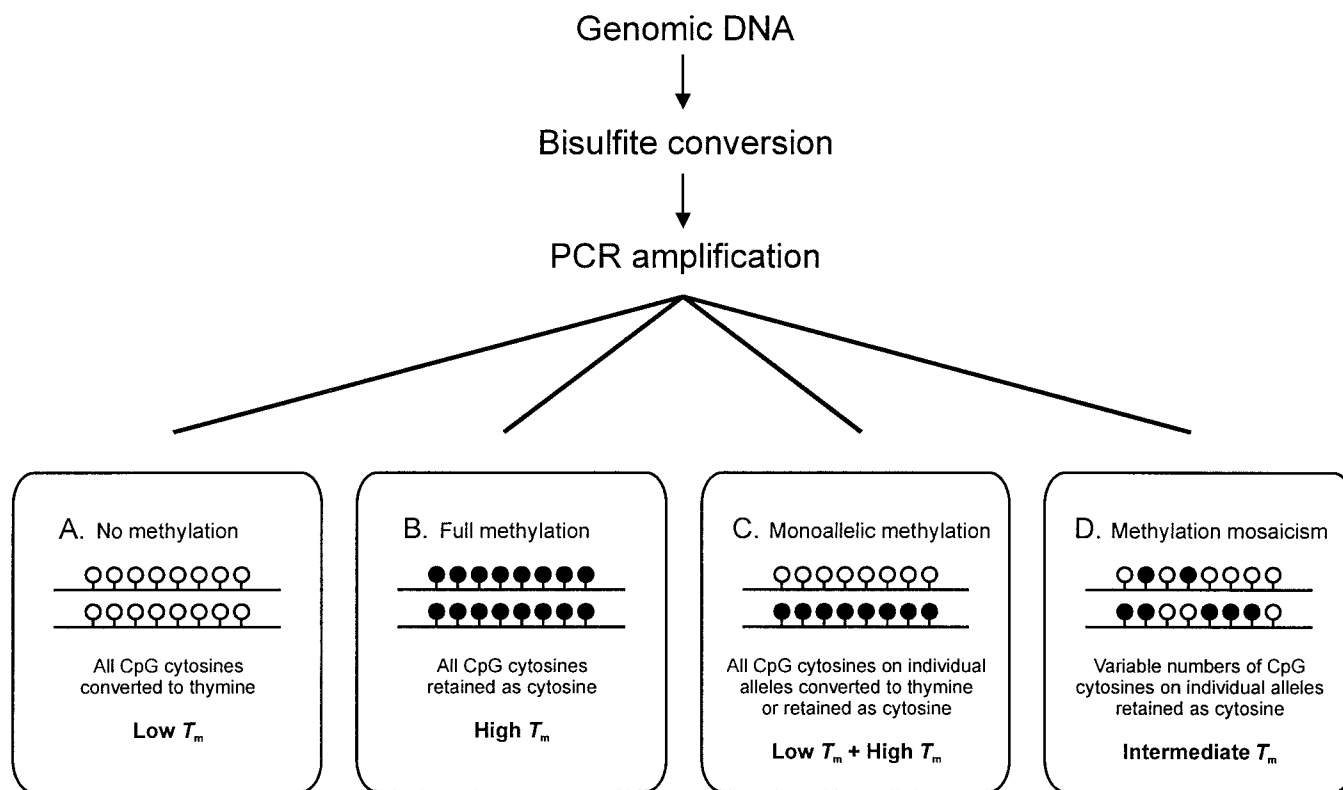


Fig. 1. Principle of melting curve analysis for resolution of DNA methylation patterns.

the PCR product will be substantially higher (Fig. 1B). If the DNA sample contains a mixture of alleles that are either unmethylated or fully methylated, amplification will yield two different PCR products with a low and a high  $T_m$ , respectively (Fig. 1C). If the target sequence exhibits methylation "mosaicism", i.e., the number of  $m^5C$ s varies among different alleles within the same sample, the PCR product represents a pool of molecules with different  $T_m$ s, leading to an overall intermediate  $T_m$  (Fig. 1D).

#### IN-TUBE MELTING CURVE ANALYSIS OF THE *SNRPN* GENE

The gene encoding *SNRPN* is a convenient model for investigating melting profiles of different allelic constellations of DNA methylation. *SNRPN* is located in an imprinting regulatory region at chromosome 15q11-q13, and its promoter is usually fully methylated (>96% of all CpG dinucleotides) on the maternal chromosome and completely devoid of methylation on the paternal chromosome (14). Two inherited developmental disorders, Prader-Willi syndrome and Angelman syndrome, are associated with large deletions, uniparental disomy or imprinting mutations of the *SNRPN* region. Healthy individuals have both methylated and unmethylated *SNRPN* alleles, whereas patients with Prader-Willi syndrome have only methylated alleles and patients with Angelman syndrome have only unmethylated alleles (16).

The melt map of a 153-bp genomic DNA region of the

*SNRPN* CpG island, including 11 CpG dinucleotides, is depicted in Fig. 2A. This region has a GC content of 67% with a predicted maximum  $T_m$  of 85 °C. Treatment with sodium bisulfite and subsequent PCR would cause the formation of two distinct noncomplementary strands with GC contents and  $T_m$ s determined by the  $m^5C$  contents of the original templates. For the antisense strand, the fully methylated sequence would have a GC content of 33% and a maximum  $T_m$  of 78 °C, whereas the unmethylated sequence would have a GC content of 26% and a maximum  $T_m$  of 66 °C (Fig. 2A).

DNA samples from an apparently healthy individual, a patient with Prader-Willi syndrome, and a patient with Angelman syndrome were treated with sodium bisulfite, and the *SNRPN* promoter CpG island was subsequently amplified and GC-clamped with primers that are specific for bisulfite-treated DNA but do not discriminate between methylated and unmethylated alleles. The melt maps of the amplification products originating from either methylated or unmethylated *SNRPN* alleles are depicted in Fig. 2B. The GC-clamped sequence containing the unmethylated *SNRPN* region has a lower-temperature melting domain with a predicted  $T_m$  of 64.9 °C, whereas the  $T_m$  of this domain is 68.3 °C for the fully methylated sequence (Fig. 2B). By conventional PCR, all samples yielded a product of the expected length and no nonspecific products (data not shown).

Melting analysis of the PCR products generated with

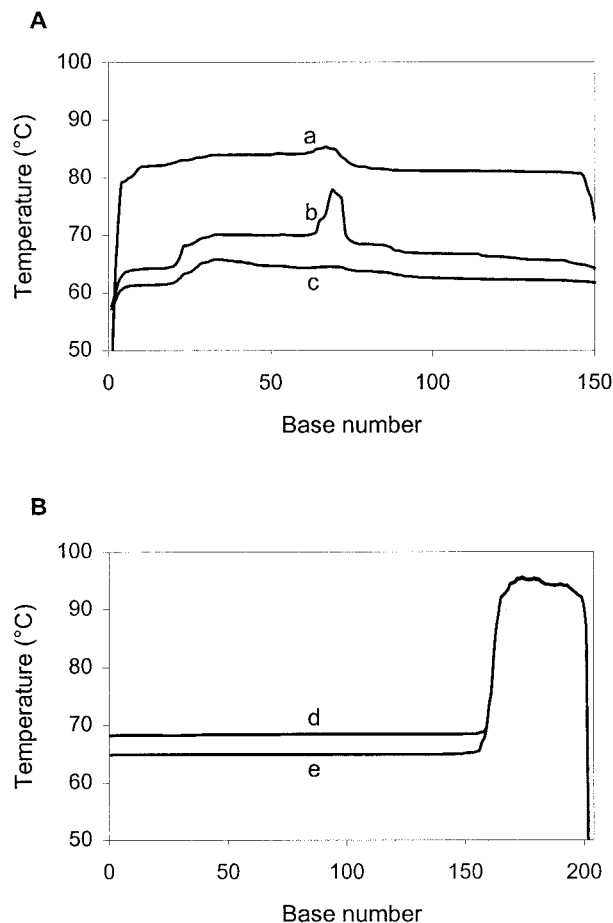


Fig. 2. Melt maps of a 153-bp region of the *SNRPN* promoter in genomic DNA (A) and a 203-bp GC-clamped *SNRPN* PCR product (B). (A), computerized melt maps of a 153-bp region of the *SNRPN* promoter in untreated genomic DNA (curve a) and DNA after treatment with sodium bisulfite (curve b, methylated lower strand; curve c, unmethylated lower strand). (B), melt maps calculated for the 203-bp GC-clamped *SNRPN* PCR product (curve d, methylated; curve e, unmethylated).

DNA from an apparently healthy individual showed a biphasic decrease in the fluorescence of the double stranded DNA dye SYBR Green I (Fig. 3A). When the melting curves were converted to melting peaks by plotting the negative derivative of fluorescence over temperature vs temperature ( $-dF/dT$  vs  $T$ ), two melting peaks were observed with apparent  $T_m$ s of 77.3 °C and 80.3 °C, respectively (Fig. 3B). With bisulfite-treated DNA from a patient with Angelman syndrome, a single melting peak was observed with an apparent  $T_m$  of 77.4 °C, whereas a single peak with an apparent  $T_m$  of 80.3 °C was obtained with DNA from a patient with Prader-Willi syndrome (Fig. 3B).

To test the reproducibility of this method, we used the *SNRPN* model to examine intertube and intersample variability. When the same *SNRPN* PCR product generated from DNA from an apparently healthy individual was distributed among seven individual glass capillaries, the  $T_m$  varied by  $\sim 0.3$  °C for both the unmethylated peak

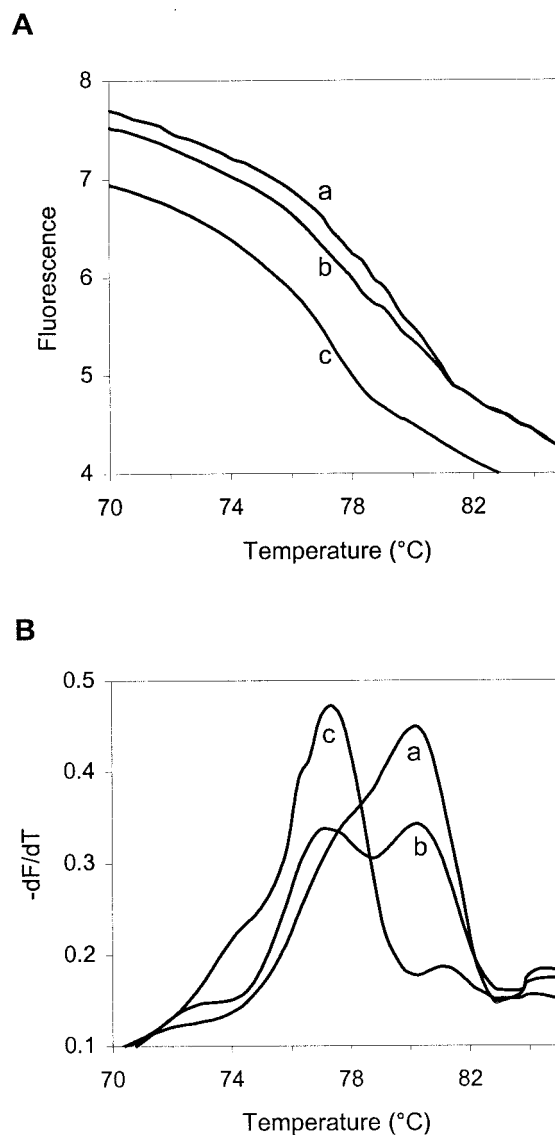


Fig. 3. Fluorescence melting curves (A) and melting peaks (B) for the *SNRPN* gene.

Bisulfite-treated DNA was amplified from a patient with Prader-Willi syndrome (A and B, curve a), an apparently healthy individual (A and B, curve b), and a patient with Angelman syndrome (A and B, curve c). Fluorescence data for melting curves were acquired by heating the PCR products from 70 °C to 98 °C at a transition rate of 0.1 °C/s in the presence of SYBR Green I. Melting peaks were obtained by plotting the negative derivative of fluorescence over temperature vs temperature ( $-dF/dT$  vs  $T$ ).

and the methylated peak. The variation in  $T_m$  was  $\sim 0.4$  °C when the same DNA template was amplified in seven independent reactions and subjected to melting curve analysis. In an additional series of experiments with DNA from four different individuals, the  $T_m$  variation was  $< 0.6$  °C, and the average  $T_m$  did not vary between experiments performed on different days. These data suggest that melting peak data are highly reproducible under fixed assay conditions and that the subtle variations in  $T_m$  can be ascribed, at least in part, to temperature differences in the sample carousel, in agreement with the technical

specification of the LightCycler system (LightCycler Operator's Manual, Ver. 3.0). Initial heating and reannealing before melting analysis, as recommended in some protocols, lead to highly variable melting profiles, probably attributable to the formation of heteroduplexes and/or hybrids between amplified DNA and excess primers (data not shown).

#### IN-TUBE DETECTION OF HETEROGENEOUS METHYLATION PATTERNS

To examine the feasibility of resolving heterogeneous methylation patterns by melting curve analysis, we examined the promoter CpG island of the  $p15^{\text{Ink4b}}$  tumor suppressor gene, which displays high intra- and interindividual variation in methylation density among patients with AML (11, 17). Bisulfite-treated DNA from AML patients and control cell lines was amplified and GC-clamped with primers flanking a region of  $p15^{\text{Ink4b}}$  that contains 27 CpG dinucleotides (11). As shown in Fig. 4, DNA from the unmethylated cell line HL-60 showed a melting peak with an apparent  $T_m$  of 81.3 °C, whereas a peak with an apparent  $T_m$  of 88.9 °C was obtained with DNA from the methylated MOLT-4 cell line. With DNA from two AML samples shown previously to contain high fractions of heterogeneously methylated  $p15^{\text{Ink4b}}$  alleles (11), melting transitions tended to broaden and the melting peaks had  $T_m$ s of 84.4 °C and 86.2 °C, respectively. Thus, in accordance with the theory (Fig. 1D), samples containing heterogeneously methylated DNA show melting peak  $T_m$ s between those of the corresponding unmethylated and fully methylated sequences.

When melting curve acquisition was integrated with PCR on the LightCycler by using the components from a commercially available reagent set, the  $p15^{\text{Ink4b}}$  melting peak profiles of HL-60 and MOLT-4 were similar to those obtained with PCR products generated on a block thermocycler (data not shown). However, the melting peaks

shifted ( $T_m = 83.6$  °C for HL-60 and  $T_m = 92.4$  °C for MOLT-4), possibly because of the different concentrations of  $\text{MgCl}_2$  and the substitution of dTTP with dUTP.

#### Discussion

We have shown that fluorescence melting curve analysis is a fast and cost-effective method that can be fully integrated with PCR for detection of aberrant DNA methylation patterns. Once the bisulfite conversion of sample DNA has been performed, screening of samples can be completed in <45 min by using standard PCR reagents. Also, considering that the risk of PCR contamination is substantially reduced because no manual transfer of PCR products is required, this method should provide an attractive alternative to traditional gel-based methylation assays.

Appropriate design of PCR primers is crucial to successful methylation resolution by melting curve analysis. First, the primers must discriminate between methylated and unmethylated alleles neither at the nucleotide level (18) nor at the amplification level (19). Furthermore, because multiple melting domains in a PCR product lead to a corresponding number of melting peaks (20), a change in the methylation status of a particular CpG dinucleotide will affect only the  $T_m$  of the melting domain in which the CpG is located. Preferably, all CpG sites of the target region should be contained in one lower-melting domain of the amplified product. Modulation of melting profiles may easily be achieved by using one of several available computer algorithms in combination with PCR-based GC-clamping (21). The MELT94 algorithm used in this study produces theoretical  $T_m$ s that are significantly lower than the experimental values, but it is very accurate in predicting the domain structure of the DNA molecule (unpublished data).

Temperature transition rates and concentrations of salt and dye may have a significant impact on the width and absolute position of a PCR product's melting peak (20, 22, 23) and must be appropriately controlled for reproducible results. For routine high-throughput applications, the temperature transition rate might be chosen as the best compromise between speed and resolution. A high transition rate may cause peak broadening that hampers differentiation between methylated and unmethylated alleles. As shown for the human *SNRPN* gene, analysis of monoallelic methylation of a region containing 11 CpG sites at a transition rate of 0.1 °C/s led to two overlapping, but easily differentiable, melting peaks with a  $T_m$  difference of ~3 °C. At this transition rate, the melting curve analysis could be completed within 4 min. Nonoverlapping melting peaks may be obtained by lowering the temperature transition rate or increasing the number of CpG sites in the target sequence.

One of the strongest features of the present method is that it can resolve heterogeneous methylation patterns. Previous studies of bone marrow samples from patients

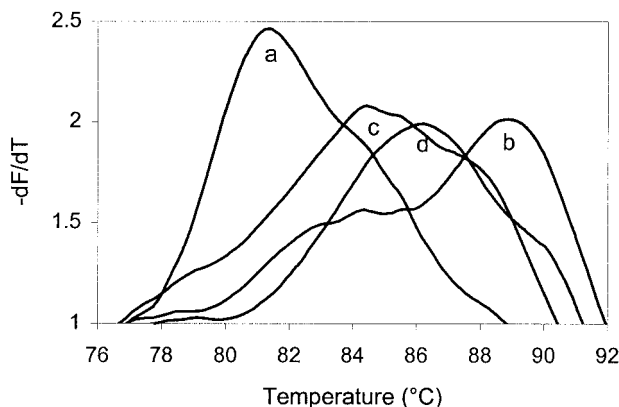


Fig. 4. Fluorescence melting peaks for the  $p15^{\text{Ink4b}}$  gene.

Bisulfite-treated DNA was amplified from two control cell lines, HL-60 (curve a, unmethylated) and MOLT-4 (curve b, fully methylated), and from bone marrow cells from patients with AML (curves c and d).

with AML have demonstrated that the content and distribution of m<sup>5</sup>C in the promoter sequences of some tumor suppressor genes may differ significantly between different cells from the same patient (11, 17, 24, 25). Furthermore, heterogeneous methylation of promoter CpG islands in noncancerous tissues has been demonstrated for the genes encoding prolactin and growth hormone (26), suggesting that this phenomenon may be more common in biologic processes than previously believed. As shown for the *p15<sup>Ink4b</sup>* gene promoter, heterogeneously methylated AML samples can be easily distinguished by melting analysis by showing a broader melting peak with an overall  $T_m$  between the  $T_m$ s of the unmethylated and fully methylated alleles. Although melting curve analysis does not provide information on the methylation status of individual alleles or individual CpGs, it is highly useful for rapid screening of samples for overall methylation status at specific genes and loci.

Recently, a methylation detection method was developed that combines MSP with real-time quantitative PCR (27, 28). The major advantages of real-time MSP over conventional MSP are the in-tube format and the quantitative dimension. The drawbacks of this method are that it requires expensive hybridization probes, calibration curves must be generated in each setting, heterogeneous methylation may not be detected, and analysis of methylated and unmethylated alleles must be performed in separate tubes. Melting curve analysis, on the other hand, does not require any expensive reagents, resolves heterogeneous methylation, and detects methylated and unmethylated alleles in the same reaction in a semiquantitative fashion. In its present form, this method is not suited for exact quantitative experiments or detection of very low levels of DNA methylation. Hence, quantitative MSP and melting curve analysis are complementary techniques that may allow comprehensive studies of DNA methylation in an in-tube format.

We thank H. Hjalmsgrim for providing us with DNA samples. This work was supported by grants from the Danish Cancer Society, the Danish Medical Research Council, and the Novo Nordisk Foundation.

### References

1. Jones PA, Laird PW. Cancer epigenetics comes of age. *Nat Genet* 1999;21:163-7.
2. Baylin SB, Herman JG, Graff JR, Vertino PM, Issa JP. Alterations in DNA methylation: a fundamental aspect of neoplasia. *Adv Cancer Res* 1998;72:141-96.
3. Feinberg AP. DNA methylation, genomic imprinting and cancer. *Curr Top Microbiol Immunol* 2000;249:87-99.
4. Wang RY, Gehrke CW, Ehrlich M. Comparison of bisulfite modification of 5-methyldeoxycytidine and deoxycytidine residues. *Nucleic Acids Res* 1980;8:4777-90.
5. Frommer M, McDonald LE, Millar DS, Collis CM, Watt F, Grigg GW, et al. A genomic sequencing protocol that yields a positive display of 5-methylcytosine residues in individual DNA strands. *Proc Natl Acad Sci U S A* 1992;89:1827-31.
6. Herman JG, Graff JR, Myohanen S, Nelkin BD, Baylin SB. Methylation-specific PCR: a novel PCR assay for methylation status of CpG islands. *Proc Natl Acad Sci U S A* 1996;93:9821-6.
7. Gonzalzo ML, Jones PA. Rapid quantitation of methylation differences at specific sites using methylation-sensitive single nucleotide primer extension (Ms-SNuPE). *Nucleic Acids Res* 1997;25:2529-31.
8. Sadri R, Hornsby PJ. Rapid analysis of DNA methylation using new restriction enzyme sites created by bisulfite modification. *Nucleic Acids Res* 1996;24:5058-9.
9. Xiong Z, Laird PW. COBRA: a sensitive and quantitative DNA methylation assay. *Nucleic Acids Res* 1997;25:2532-4.
10. Wittwer CT, Ririe KM, Andrew RV, David DA, Gundry RA, Balis UJ. The LightCycler: a microvolume multisample fluorimeter with rapid temperature control. *Biotechniques* 1997;22:176-81.
11. Aggerholm A, Guldborg P, Hokland M, Hokland P. Extensive intra- and interindividual heterogeneity of *p15<sup>INK4B</sup>* methylation in acute myeloid leukemia. *Cancer Res* 1999;59:436-41.
12. Zeschnick M, Lich C, Buiting K, Doerfler W, Horsthemke B. A single-tube PCR test for the diagnosis of Angelman and Prader-Willi syndrome based on allelic methylation differences at the *SNRPN* locus. *Eur J Hum Genet* 1997;5:94-8.
13. Lerman LS, Silverstein K, Fripp B, Sauer P, Dresselhaus C. Melt program. <http://web.mit.edu/osp/www/melt.html>.
14. Zeschnick M, Schmitz B, Dittrich B, Buiting K, Horsthemke B, Doerfler W. Imprinted segments in the human genome: different DNA methylation patterns in the Prader-Willi/Angelman syndrome region as determined by the genomic sequencing method. *Hum Mol Genet* 1997;6:387-95.
15. Guldborg P, Grønboek K, Aggerholm A, Platz A, thor Straten P, Ahrenkiel V, et al. Detection of mutations in GC-rich DNA by bisulphite denaturing gradient gel electrophoresis. *Nucleic Acids Res* 1998;26:1548-9.
16. Nicholls RD, Saitoh S, Horsthemke B. Imprinting in Prader-Willi and Angelman syndromes. *Trends Genet* 1998;14:194-200.
17. Dodge JE, List AF, Futscher BW. Selective variegated methylation of the p15 CpG island in acute myeloid leukemia. *Int J Cancer* 1998;78:561-7.
18. Clark SJ, Harrison J, Paul CL, Frommer M. High sensitivity mapping of methylated cytosines. *Nucleic Acids Res* 1994;22:2990-7.
19. Warnecke PM, Stirzaker C, Melki JR, Millar DS, Paul CL, Clark SJ. Detection and measurement of PCR bias in quantitative methylation analysis of bisulphite-treated DNA. *Nucleic Acids Res* 1997;25:4422-6.
20. Wartell RM, Benight AS. Thermal denaturation of DNA molecules: a comparison of theory with experiment. *Phys Rep* 1985;126:67-107.
21. Sheffield VC, Cox DR, Lerman LS, Myers RM. Attachment of a 40-base-pair G+C-rich sequence (GC-clamp) to genomic DNA fragments by the polymerase chain reaction in improved detection of single-base changes. *Proc Natl Acad Sci U S A* 1989;86:232-6.
22. Hillen W, Goodman TC, Wells RD. Salt dependence and thermodynamic interpretation of the thermal denaturation of small DNA restriction fragments. *Nucleic Acids Res* 1981;9:415-36.
23. Ririe KM, Rasmussen RP, Wittwer CT. Product differentiation by analysis of DNA melting curves during the polymerase chain reaction. *Anal Biochem* 1997;245:154-60.
24. Cameron EE, Baylin SB, Herman JG. p15 (INK4B) CpG island methylation in primary acute leukemia is heterogeneous and suggests density as a critical factor for transcriptional silencing. *Blood* 1999;94:2445-51.
25. Melki JR, Vincent PC, Clark SJ. Concurrent DNA hypermethylation

- of multiple genes in acute myeloid leukemia. *Cancer Res* 1999; 59:3730–40.
- 26.** Ngô V, Gourdjji D, Laverriere JN. Site-specific methylation of the rat prolactin and growth hormone promoters correlates with gene expression. *Mol Cell Biol* 1996;16:3245–54.
- 27.** Eads CA, Danenberg KD, Kawakami K, Saltz LB, Blake C, Shibata D, et al. MethyLight: a high-throughput assay to measure DNA methylation. *Nucleic Acids Res* 2000;28:e32.
- 28.** Lo YM, Wong IH, Zhang J, Tein MS, Ng MH, Hjelm NM. Quantitative analysis of aberrant p16 methylation using real-time quantitative methylation-specific polymerase chain reaction. *Cancer Res* 1999;59:3899–903.